

Predictions about cosmic ray emission from evolutionary synthesis models

M. Cerviño¹, R. Diehl¹, D. H. Hartmann², J. Knödseder³, K. Kretschmer¹, and S. Plüschke¹

¹Max-Planck-Institut für extraterrestrische Physik, 85740 Graching, Germany

²Physics & Astronomy Dep., Clemson Univ. Clemson, SC29634, USA

³Centre d'Etude Spatiale des Rayonnements, CNRS/UPS, B.P. 4346, 31028 Toulouse Cedex 4, France

Abstract. We have extended our evolutionary synthesis models for star forming regions to the γ -ray domain. We obtain the light-curves of γ -ray line emission due to radioactive decay of stellar nucleosynthesis products, such as ^{26}Al , ^{60}Fe , or the e^-e^+ annihilation line as well as the evolution of the kinetic energy from massive stars. We present the correlation of these lines with the ionizing flux produced by massive stars and some preliminary predictions about the Cosmic Ray production in star forming regions. We show that the predicted γ -ray line observations combined with others multi-wavelength measurements can efficiently constrain the age of a stellar population, and help to identify the primary nucleosynthesis sources of the radio-isotopes.

1 Introduction

Massive stars via stellar winds and Supernova explosions (SNe) produce the ejection of new elements into the Interstellar Medium (ISM). They are also responsible for the input of kinetic energy and structure formation in the ISM. Hence, they are the primary source of a hot phase of the ISM that produces γ -ray emission due to the decay of radioactive isotopes as well as cosmic rays. The star formation sites where massive stars are found can be study by the use of evolutionary synthesis models for star forming regions. Such models have been proved to be a useful tool for the study of the UV and Optical emission of extragalactic H II regions where a large amount of gas, typically about $10^5 M_\odot$, has been transformed into stars (Mas-Hesse & Kunth 1999). In the case of our Galaxy, such massive OB associations have been not observed, and statistical effects due to the small number of stars may produce a large dispersion in the observed associations when they are compared to model outputs.

In the last years, several efforts have been performed to predict the γ -ray emission in galactic OB associations and stellar clusters in on the of synthesis models (e.g. Plüschke et

al. 2001, Cerviño et al. 2000). Such models are able to predict the γ -ray flux from some radio-isotopes (^{26}Al and ^{60}Fe in particular) as well as the expected emission of the e^-e^+ annihilation line from the integration (analytical and numerical, respectively) of the properties of individual stars. Moreover, as far as the synthetic stellar populations are known, models are able to predict the relation between the γ -emission lines with the emission at other wavelengths. With such models are also possible estimate the stadistical effects due to the discreteness of the stellar populations of Galactic associations in terms either confidence limits of the output results (using Monte Carlo simulations) or relative dispersions (using Monte Carlo or Analytical/Numerical simulations).

In this contribution we present the theoretical Supernova rate, SNr, kinetic power, P_k , and the expected flux of some radio-isotopes and the e^-e^+ annihilation line. We also show the mean energy per nucleon of ^{12}C and ^{16}O resulting from the energy input of stellar winds and supernovae explosions. We discuss the ratio ^{26}Al line over the ionizing flux, Q_0 , and the ration of the 1.809 MeV luminosity over the total kinetic energy. Both ratios can be used to identify the primary nucleosynthesis sources of the radio-isotopes. Finally we estimate the uncertainty due to the discreteness of the stellar populations.

2 Kinetic power, SNr, ^{26}Al and ^{60}Fe γ -emission lines, and the e^-e^+ annihilation line

In this work we have use an updated version of the synthesis code presented in Cerviño et al. (2000). We have use the evolutionary tracks by Meynet et al. (1997) with solar metallicity and enhanced mass lost rates. For the presented results we use a power-law Initial Mass function (IMF) with a slope equal to the Salpeter value in the mass range $2 - 120 M_\odot$. An instantaneous burst of star formation has been assumed. We have used the SN yields from Woosley & Weaver (1995) for stars that do not reach the Wolf-Rayet (WR) phase and the yields form Woosley et al. (1995) for WR stars.

The resulting SNr, normalized to the total mass of the cluster, is shown in Fig. 1. The stars in the mass range $50 - 120 M_{\odot}$ explode almost instantaneously at 4 Myr for this set of tracks and produce a peak. Later, the SNr decreases slowly.

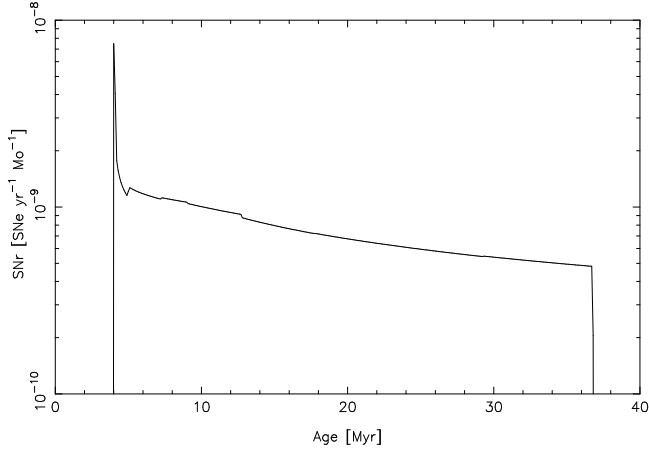


Fig. 1. Temporal evolution of the predicted SNr.

The contribution of the kinetic power from each star, p_k , to the total kinetic power, P_k , is $p_k = \frac{1}{2} \dot{M} v_{\infty}^2$ where \dot{M} is the mass lost rate and v_{∞} the terminal velocity obtained from the instantaneous luminosity and effective temperature following Leitherer & Heckman (1995). The contribution from each star has been weighted with the IMF in order to obtain the P_k . For the contribution of SN, we have used the values of the kinetic energy tabulated by Woosley & Weaver (1995) and Woosley et al. (1995). The total kinetic energy has been divided by the used time step in order to obtain the kinetic power. The resulting evolution of the total kinetic power (winds + SNe) is showed in Fig. 2.

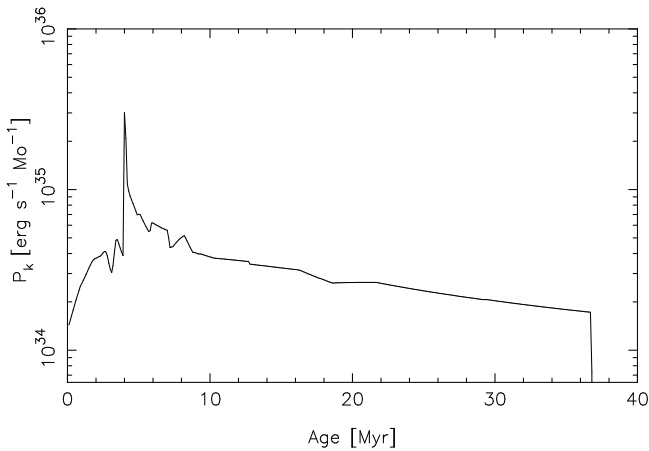


Fig. 2. Temporal evolution of the predicted kinetic power.

We have also obtained the expected 1.809 MeV and 1.173/1.332 MeV luminosity from the ^{26}Al and ^{60}Fe decays respectively. The method has been described in Cerviño et al. (2000) and we refer to this reference for further details¹.

¹A recent examination of the code outputs (Cerviño et al. 2001)

In Fig. 3 we show the temporal evolution of the luminosities normalized to the mass of gas transformed into stars in the synthetic cluster. The figure shows that a star forming region reach a peak in the 1,809 MeV luminosity at the time when massive WR stars are present (from 3 to 4 Myr) and slowly decay for larger ages: the lower the initial mass, the lower the production of ^{26}Al in the SN explosion. The 1.173/1.332 MeV luminosity shows a more constant behavior until ~ 19 Myr as far as the SN yields do not present the strong dependence with mass than the ^{26}Al ones. For larger ages (i.e. initial masses lower than $12 M_{\odot}$) the 1.173/1.332 MeV luminosity (and the ^{60}Fe yield) decreases monotonically until 38 Myr when the SNe activity disappear in the cluster.

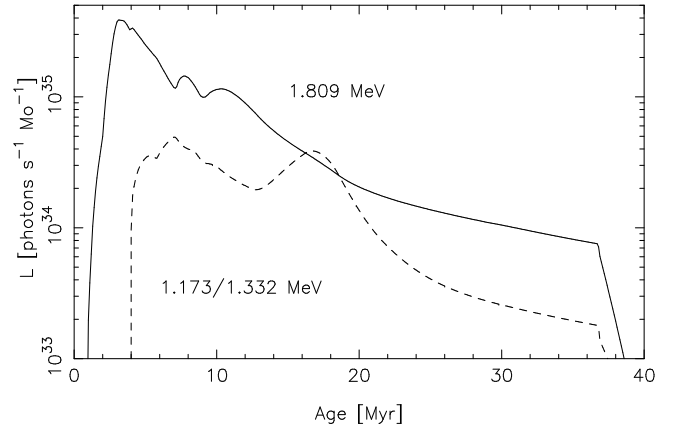


Fig. 3. Temporal evolution of the predicted 1.809 MeV and 1.173/1.332 MeV luminosity from the ^{26}Al and ^{60}Fe decays respectively.

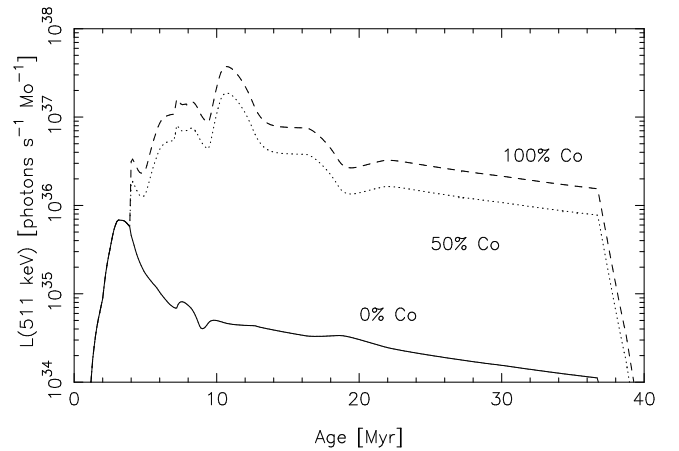


Fig. 4. Temporal evolution of the predicted 511 keV luminosity for different escape fractions of positrons produced by ^{56}Co decay.

Finally, we have computed the predicted 511 keV luminosity taken into account the radioactive decay of ^{22}Na (with a branching ratio for the formation of e^+ of 0.905), ^{26}Al shows that the use of the mass lost rate in the computation of the yields may lost some rapid evolutionary phases. We show here the new results, that have only small differences respect to the previous ones

(0.85), ^{44}Ti (0.95), ^{56}Co (0.19). A mean-life of 5×10^5 years has been assumed for the e^+ and the annihilation process has been corrected by a factor 0.575 that takes into account that each e^+ produce two 511 keV photons with a efficiency of 28.75%, whereas the other 71.25% produces continuum luminosity. In Fig. 4 we show the temporal evolution of the predicted 511 keV luminosity for different escape fractions of positrons produced by ^{56}Co decay. The mean-life of the ^{56}Ni in the chain $^{56}\text{Ni} \rightarrow ^{56}\text{Co} \rightarrow ^{56}\text{Fe} + e^+$ is 111 days. At this time it is not clear if the e^+ produced can escape of the SN envelope or if they decay inside.

3 Mean input energy per nucleon of ^{12}C and ^{16}O

We have also computed the mean input energy per nucleon, $\langle E \rangle$, of ^{12}C and ^{16}O . We have assumed that, for each star in the cluster, the kinetic power of a nucleon is the total kinetic power produced by the star and multiplied by the mass fraction of the nucleon in the surface of the star. We have also computed the total mass loss of each element. The mean energy per nucleon has been obtained from the ratio of the kinetic power and the total mass loss weighted with the IMF. The results are showed in Fig. 5 The discontinuity at 7 Myr is due to the transition between WR and no-WR SNe. The figure shows that the mean energy per nucleon becomes higher for older ages. It can be understood taking into account that the kinetic energy released in each explosion (about 10^{51} erg) is almost constant without dependence with the mass. But the lower the initial mass of the progenitor, the lower the amount of ejected material in the explosion. The combination of both effects produce more energetic particles for lower initial mass of the SN progenitor.

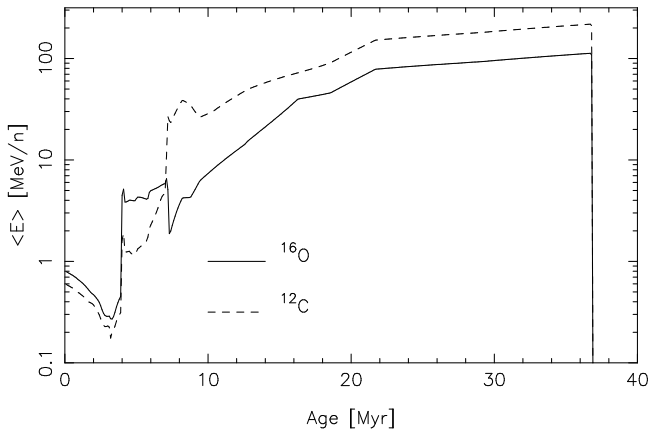


Fig. 5. Temporal evolution of the predicted mean energy per nucleon for ^{12}C and ^{16}O ions.

4 Equivalent O7 V star yields, Y_{26}^{O7V} and $L(1.809 \text{ MeV})$ over E_k ratio.

Based in the observed proportionality of the 1.809 MeV γ -line with the radio-thermal emission, Knoödlseder (1999) in-

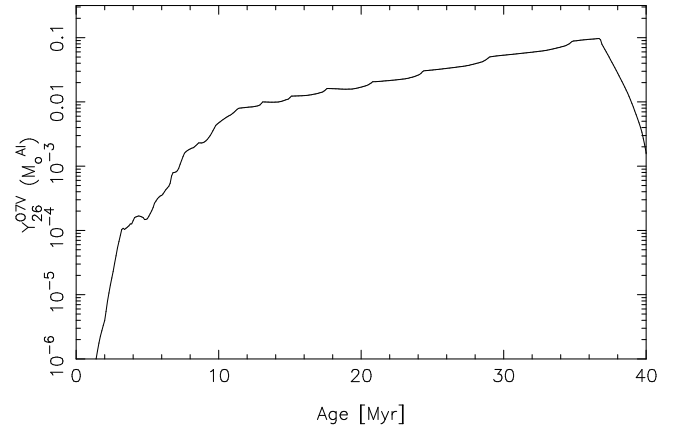


Fig. 6. Temporal evolution of the predicted Y_{26}^{O7V} ratio.

roduced the *equivalent O7 V star ^{26}Al yield*, Y_{26}^{O7} , as the ratio of the mass of ^{26}Al active in the cluster over the ionizing luminosity normalized to the one of a O7 V star ($\log Q_0^{\text{O7V}} = 49.05 \text{ ph s}^{-1}$). Such a ratio has the advantage to be independent of the mass normalization, i.e. the obtained values can be tested with the observation of any system whatever the mass transformed into stars is.

The evolution of Y_{26}^{O7V} is shown in Fig. 6. Four phases can be found: (i) stellar wind phase up to 3 Myr with a steep rise of the ratio, (ii) Type Ib/c supernova phase (from WR stars) from 3 to 7 Myr with a faltering of the slope, (iii) Type II supernova phase from 7 to 37 Myr with a step around 7 Myr and a tail of positive slope, and iv Decay phase, after 37 Myr. Note that the ratio vary in more that 4 orders of magnitude during the evolution of the cluster and it is not very dependent on the value of the IMF slope. So, Y_{26}^{O7V} becomes a useful parameter to constrain the age of the burst, or, if the age is know by other methods (observations in other wavelengths), constrain the contribution of massive stars to the observed mass of ^{26}Al . As an example, the value of Y_{26}^{O7V} obtained for the Cygnus region is about 1×10^{-4} , such a value is in accord with our models predictions if the region is dominated by a cluster formed 4–6 Myr ago.

In Fig. 7 we show the ratio of the luminosity of the 1.809 MeV line and the integrated kinetic energy, E_k , released by the cluster. In this case, the kinetic energy increases with time and, so, the ratio decreases. Again, this ratio is independent on the mass transformed into stars and can be used for any cluster whatever the mass. The E_k value is directly related with the radius of the (super)bubble formed by the star formation process (with the corresponding corrections due to radiative energy losses in the structure formation) and it can be obtained by optical ($\text{H}\alpha$ filaments) or radio (HI emission) observations. The ratio varies over three orders of magnitude during its evolution and can be also used to constrain the age of the stellar cluster, and together with Y_{26}^{O7V} and other outputs, to test the self-consistency of the predictions.

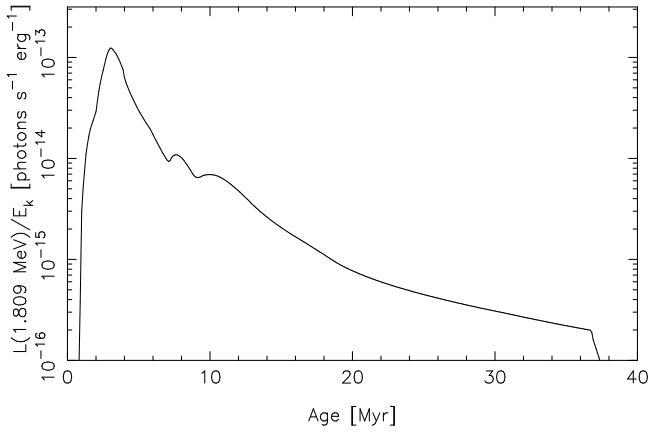


Fig. 7. Temporal evolution of the predicted $L(1.809 \text{ MeV})$ over E_k ratio.

5 Uncertainties due to the discreteness of the stellar population.

The dispersion due to the discreteness of stellar populations (as the ones that Monte Carlo simulations includes) must be considered when the output of a synthesis code is compared with real stellar populations. Such a dispersion can also be obtained analytically using the prescriptions of Buzzoni (1989, see also Cerviño 2001b). As an example, we show in Fig. 8 the probability density function of the Y_{26}^{O7V} obtained from 1000 Monte Carlo simulations of 100 stars in the mass range $8 - 25 M_{\odot}$ assuming a Salpeter IMF slope. Fig. 9 shows the relative dispersion obtained analytically in units of $M_{\odot}^{-0.5}$, where M is the amount of mass transformed into stars in the cluster. The figures show that a considerable dispersion at the early evolution due to the small number statistics at the high-mass end. During the subsequent evolution, the relative uncertainty is roughly constant, with a minimum around 5 – 10 Myr followed by a slight rise of the uncertainty with time.

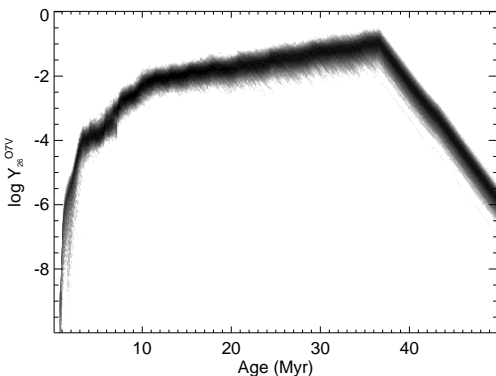


Fig. 8. Probability density functions of Y_{26}^{O7V} for a set of 1000 Monte Carlo simulations.

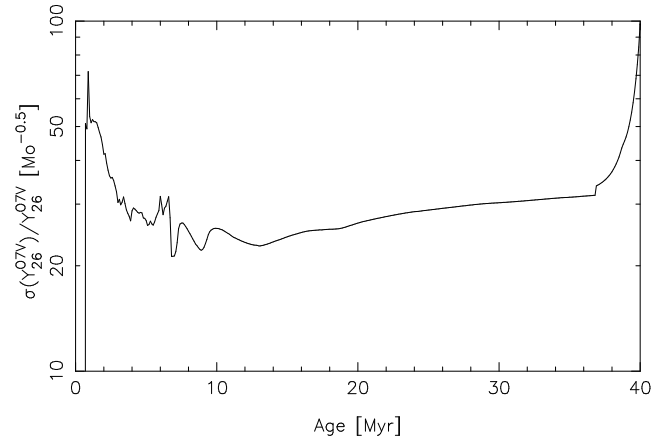


Fig. 9. Analytical relative error of Y_{26}^{O7V} in units of $M_{\odot}^{-0.5}$.

6 Conclusions

In this contribution we have shown properties related with γ -emission lines based in the computations of evolutionary synthesis codes. We have shown that such codes present the advantage of allowing to obtain correlations with other wavelength ranges and constrain the evolutionary status of the studied systems and the relative relevance of star formation processes in the γ -line emission. Any case, the dispersion due to the discreteness of stellar populations in the observed systems must be taken into account in any comparison with real data. We have also shown that the use of ratios of different quantities better constrain the physical properties of the systems. We extend this work to find more correlations with other observed quantities (individual stellar populations, X-ray emission and optical emission lines) and to better constrain the physical properties of the systems where the models can be applied.

Acknowledgements. MC acknowledges the MPE for financial support.

References

- Buzzoni, A. 1989, *ApJS*, 71, 871
- Cerviño, M., Knödseder, J., Schaerer, D., von Ballmoos, P. & Meynet, G. 2000, *A&A*, 363, 970
- Cerviño, M., Knödseder, J., Gómez-Flechoso, M.A., Castander, J., Mollá, M., Luridiana, V. and Schaerer, D. 2001, *A&A*. (submitted)
- Cerviño, M., Vals-Gabaud, D., Luridiana, V., and Mas-Hesse, J.M., 2001b, *A&A* (submitted)
- Knödseder, J., 1999, *ApJ*, 510, 915
- Mas-Hesse, J.M. & Kunth, D. 1999, *A&A* 349, 765
- Leitherer, C. and Heckman, T., 1995, *ApJS*, 96, 9
- Meynet, G., Arnould, M., Prantzos, N., and Paulus, G., 1997, *A&A*, 320, 460
- Plüschke, S., Diehl, R., Hartmann, D.H. and Oberlack, U., 2001, *A&A*, submitted (astro-ph/0005372)
- Woolsey, S.E., Langer, N., and Weaver, T., 1995, *ApJ*, 448, 315
- Woolsey, S.E., and Weaver, T., 1995, *ApJS*, 101, 181